Impact of lens distortions on strain measurements obtained with digital image correlation

P. Lava[1], W. Van Paepegem[2], S. Coppieters[1], I. De Baere[2] and D. Debruyne[1,3]

[1]Catholic University College Ghent , Association K.U. Leuven
Department of Mechanical Engineering, Gebroeders Desmetstraat 1, B-9000 Gent
pascal.lava@kahosl.be

[2]Department of Materials Science and Engineering, Ghent University,
St-Pietersnieuwstraat 41, B-9000 Gent

[3]Department MTM, Katholieke Universiteit Leuven,
Kasteelpark Arenberg 44, B-3001 Leuven (Heverlee)

ABSTRACT

The determination of strain fields based on displacements obtained via DIC at the micro-strain level is still a cumbersome task. In particular when high-strain gradients are involved, e.g. in composite materials with multidirectional fibre reinforcement, uncertainties in the experimental setup and errors in the derivation of the displacement fields can substantially hamper the strain identification process. In this contribution, the aim is to investigate the impact of lens distortions on strain measurements. To this purpose, we first perform pure rigid body motion experiments, revealing the importance of precise correction of lens distortions. Next, a uni-axial tensile test on a textile composite with spatially varying high strain gradients is performed, resulting in very accurate determined strains along the fibers of the material.

1 Introduction

Optical full-field measurement methods such as Digital Image Correlation (DIC) are currently extensively applied to study the deformation characteristics of a wide range of materials [1, 2, 3]. Moreover, the understanding of the complex structural deformation behavior of fibre reinforced composites is often based on local strain analysis [4]. The measured strain fields, however, are concentrated at the micro-strain level resulting in high uncertainties due to the experimental setup and errors in the derivation of the displacement fields. Nothwithstanding, an excellent control on the accuracy and precision of the obtained displacement and strain results is a clear prerequisite before one can embark on e.g. the identification of material parameters via inverse methodology.

In the past, various numerical studies have been performed to validate the accuracy of DIC displacement and strain fields [5, 6, 7, 8, 9]. The impact of out-of-plane motion on 2D and 3D digital image correlation measurements has been intensively investigated in Ref.[10], whereas the influence of lens distortions on the measured displacement fields was studied in Ref.[11]. Few attention, however, has been paid to the impact of lens distortions on the determined strain fields, which will be the subject of this contribution.

Experiments performed in view of material characterization are often in-plane and accordingly involve a single camera setup (2D-DIC). This has several advantages compared to a stereo camera setup, as e.g. (a) reduction in costs (only one camera involved) and (b) more precise (no cross-camera matching and triangulation). A clear disadvantage, however, is the perpendicularity requirement making the experimental setup more cumbersome. Since no triangulation procedures are involved in 2D measurements, the camera calibration setup is often omitted and with this also the correction for lens distortions in the 2D matching process. A stereo camera setup, on the other hand, urges the input of camera parameters in order to reconstruct the shapes involved. As such, corrections for lens distortion are naturally involved.

One could argue that the influence of lens distortion can be neglected by using an appropriate combination of a CCD camera and lens. This is, however, not always possible or a distortion-free system is too expensive. In addition, modern lens systems are subject to distortions down to a very small level. As such, one can expect that the impact of distortions at large deformations inducing plastic strains is neglectible. In this contribution, however, we focus on brittle materials with strain fields concentrating at the micro-strain level. In these experiments, the influence of even small distortion defects can be substantial.

In this contribution, we will undistort the determined displacement fields in single camera experiments via our inhouse DIC system MatchID [12]. In order to study the impact of this correction, we first perform pure rigid body motion experiments. Various lenses of different distortion magnitude are investigated. Next, a uni-axial tensile test on a textile composite with spatially varying high strain gradients is performed.

The outline of this article is as follows. In Sec. 2 we present the formalism for lens distortion determination and corrections. Our results are included in Sec. 3. We conclude in Sec. 4.

2 Formalism

In this section we briefly outline the procedure that is implemented to account for lens distortions in our correlation algorithms. In addition, we summarize how the distortion parameters for a specific setup are obtained.

2.1 Lens distortions

Lens distortions have several mathematical forms, depending upon the type being modeled. Amongst these, we recognize spherical, coma , astigmatism, curvature of field, linear, decentering and radial distortions. In general, an image distortion model is given as a distortion vector D from the undistorted image coordinates to the distorted ones:

$$\mathbf{X^d} = \mathbf{X^u} + \mathbf{D}(\mathbf{X^u}, \kappa_\mathbf{i}) \ , \tag{1}$$

with $\mathbf{X^d} = (X^d, Y^d)$ and $\mathbf{X^u} = (X^u, Y^u)$ referring to the distorted and undistorted sensor positions in the pinhole camera model, respectively, and $\kappa_i (i = 1, ..., N)$ representing the distortion parameters for the model. In this contribution, only the impact of the radial distortions is investigated. Accordingly, the distortion vector D reads

$$\mathbf{D}(\mathbf{X^u}, \kappa) = \kappa_1 \rho^3 \mathbf{e_r} + \kappa_2 \rho^5 \mathbf{e_r} + \kappa_3 \rho^7 \mathbf{e_r} \ , \tag{2}$$

with

$$\rho = \sqrt{[(X^u - c_x)^2 + (Y^u - c_y)^2]} \tag{3}$$

the radial distance of the point (X^u, Y^u) relative to the image plane center location and $\mathbf{e_r}$ the radial unit vector. The coefficients for radial distortion have units pixels^{-2},pixels^{-4} and pixels^{-6}, respectively.

As can be inferred from Eq.(1), the distortion map relies on the unknown undistorted sensor locations and accordingly, can not directly be determined. In this contribution an iterative optimized Levenberg-Marquardt procedure is used to determine the corrected coordinates from the distorted ones.

2.2 Camera calibration

As discussed above, lens distortion corrections urge the input of camera calibration parameters. These are determined via a bundle adjustment technique as outlined in Ref.[13, 14], using various images of a translated and rotated planar regular grid pattern. Within a Levenberg-Marquardt optimization routine, the differences between the measured sensor coordinates and the model predictions of these locations are minimized. As such, one arrives at the following set of intrinsic and extrinsic parameters:

- $(c_x, c_y)[pixels]$: image plane center location for each camera
- $(f_x, f_y)[pixels]$: focal lengths in horizontal and vertical directions for each camera
- $f_s[pixels]$: accounting for skewing of sensor array
- $\kappa_1, \kappa_2, \kappa_3$: radial distortion coefficients

- (T_x, T_y, T_z): translation components to transform origin of camera 1 to origin of camera 2
- (θ, ϕ, ψ): relative orientation of camera 2 with respect to camera 1, representing a rotation around the X-,Y- and Z-axis, respectively.

Determining the camera parameters, however, is a numerical cumbersome task, with various error sources. Notwithstanding, an accurate camera parameter determination is of crucial importance in view of precise DIC displacement fields. It is not the purpose of this contribution, however, to perform a scrutinized estimation of errors involved with the calibration process.

3 Results

The goal of this research, i.e. the impact of lens distortion corrections on strain field measurements, is part of a broader work aiming to improve the accuracy of DIC strain measurements on fibre reinforced composites [15]. Before imposing loading conditions on specimens composed of these materials, we first subject them to pure translational and rotational motion. Deviations from zero can give an indication of the errors on the strain fields at the micro-strain level. We stress, however, that when larger plastic deformations are involved more complicated (numerical) experiments should be performed in order to quantify the errors of the large plastic strains [6]. The composite materials in this contribution, however, are very brittle with strain values concentrated at the micro-strain level justifying the use of the rigid body approach. In Fig.1 the random speckle pattern is displayed.

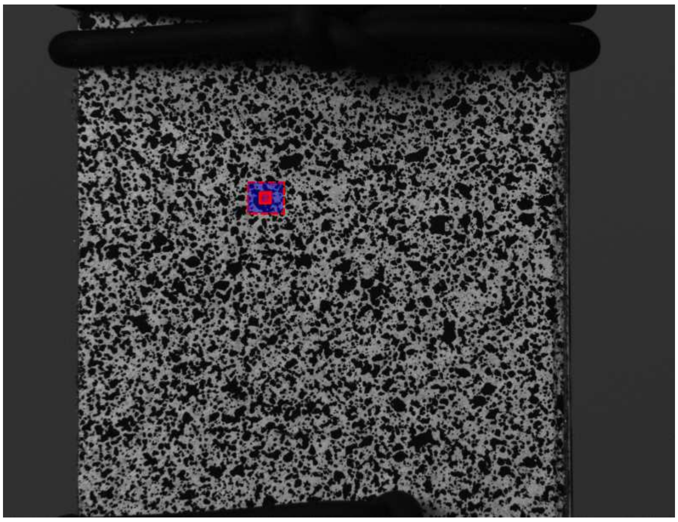

Figure 1: Speckle pattern used in the rigid body experiments. The red square represents a subset of 25×25 pixels^2, whereas the blue square shows a strain window area of 9×9 displacement data points.

Fig.2 shows the measured strains due to 1 mm rigid body translation. The experiment is performed with a stereo camera setup with one camera perpendicular to the specimen plane. Accordingly, we can mutually compare the results of 2D DIC and stereovision DIC. Both cameras are equipped with a Schneider-Kreuznach Cinegon 12mm 1.4 lens. A calibration procedure as described in Sec.2 results in normalized radial distortion parameters $\kappa_1 = -0.26236$ and $\kappa_1 = -0.22926$ for the perpendicular and angled camera, respectively. Higher order calibration parameters are omitted. A statistic binning procedure [16] allows to express the number of points as a function of strain errors for both maximum and minimum principal strain. As can be inferred, for both 2D and 3D DIC measurements the impact of the inclusion of lens distortion corrections for these specific lenses is substantial, improving the accuracy of DIC down to the 500 micro-strain level.

All results presented are obtained with the following standard DIC implementations [5, 6]: subset size 25×25 pixels^2 , step size 5 pixels, strain window 9×9 displacement data points, bicubic interpolation. The subset and strain-window sizes are reflected in Fig.1 in order to have an idea about the magnitude of these values as a function of the resolution and speckle pattern. Obviously, a larger strain window would largely improve on the strain accuracy and precision. This is, however, not an option since a tensile test on fibre reinforced material will result in high strain gradients at the micro-strain level and a too large strain window would not be able to capture these since too much smoothing is involved.

It is important to note that this involves a very basic setup in a standard laboratory environment, with no specific attention towards lighting conditions and vibrations. The slight shift between the 2D and 3D results is due to small defects in the perpendicular alignment of the camera. This is in accordance with the results of Ref.[10], stressing the importance of out-of-plane motion deformations in single camera experiments.

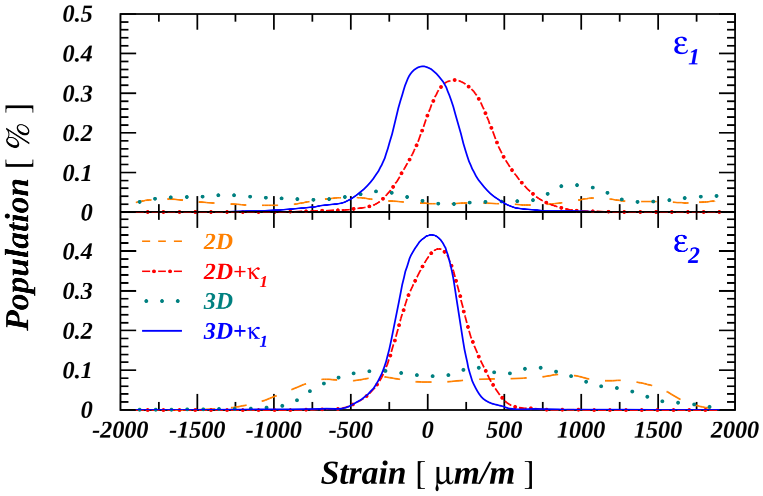

Figure 2: Impact of lens distortion corrections on the strain errors involved in a 1 mm translation experiment with a Schneider-Kreuznach Cinegon 12mm 1.4 lens. Results show the population as a function of measured strain for both maximum and minimum principal strain fields. The dashed and dotted lines correspond to uncorrected single and stereo camera results, respectively, whereas the dot-dashed and full lines reflect the impact of lens distortion corrections.

Fig.3 displays the single camera strain errors in a 1 mm translation and 2 degree in-plane rotation experiment. Here, the camera is equipped with a Schneider-Kreuznach Xenoplan 23 mm 1.4 lens yielding a normalized radial distortion parameters $\kappa_1 = -0.1873$. As can be inferred, for both experiments the impact of lens distortions is substantial, improving the accuracy down to the 200 micro-strain level.

Finally, the fibre reinforced specimen is subject to a uni-axial tensile test and measured with a single camera experiment in the exact same setup of the results of Fig.3. In Fig.4 (no distortion corrections) and Fig.5 (distortion corrections) the longitudinal strain field is displayed corresponding to a load of $F \approx 35kN$. As can be inferred, a nice strain pattern is reproduced, reflecting the strain fields along the fibers of the material. The uncorrected results, however, have an inherent gradient, whereas this is clearly removed by introducing lens distortions in this 2D setup. The strain fields have an average magnitude of 10000 $\mu m/m$. In view of the obtained strain accuracy of $\approx 200\mu m/m$ we can approach these results with confidence. A more qualitative comparison will be presented in Ref.[15].

4 Conclusions

In this contribution, we investigated the impact of lens distortions on the accuracy of strain field measurements in both single and stereo camera experiments. In order to quantify the accuracy of DIC in strain measurements at the micro-strain level we performed rigid body motion experiments. It is shown that the impact of distortion corrections is substantial improving the accuracy up to 200 micro-strain. Next, a uni-axial tensile test on a fibre reinforced composite material is performed inducing high strain gradients at the micro-strain level. A much better description of the deformations involved is obtained when distortion corrections are introduced. Accordingly we recommend to perform a camera calibration and an appropriate lens distortion compensation in single camera experiments focussing on in-plane deformation measurements at the micro-strain level.

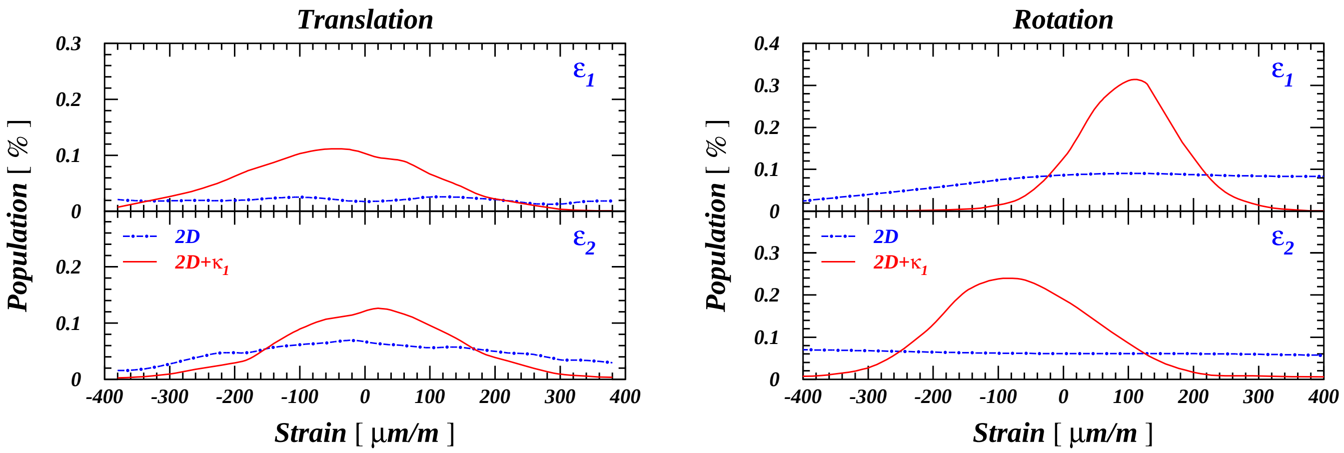

Figure 3: Impact of lens distortion corrections on the strain errors involved in a 1 mm translation (left panel) and a 2 degree rotation (right panel) experiment with a Schneider-Kreuznach Xenoplan 23 mm 1.4 lens.Results show the population as a function of measured strain for both maximum and minimum principal strain fields. The dot-dashed (full) line show the results of a single camera measurement with (without) lens distortion corrections.

References

[1] Coppieters S, Cooreman S, Sol H, Van Houtte P, Debruyne D, Identification of the post-necking hardening behaviour of sheet metal by comparison of the internal and external work in the necking zone, Journal of Materials Processing Technology 211 (2011): 545-552.

[2] Van Paepegem W, Shulev AA, Roussev IR, De Pauw S, Degrieck J, Sainov VC, Study of the deformation characteristics of window security film by digital image correlation techniques, Optics and Lasers in Engineering 47 (2009) 390-397.

[3] Rossi M, Pierron F, On the use of simulated experiments in designing tests for material characterization from full-field measurements, International Journal of Solids and Structures 49 (2012) 420-435.

[4] Daggumati S, Voet E, Van Paepegem W, Degrieck J, Xu J, Lomov SV, Verpoest I, Composites Science and Technology 71 (2011) 1171-1179.

[5] Lava P, Cooreman S, Coppieters S, De Strycker M, Debruyne D, Assessment of measuring errors in DIC using deformation fields generated by plastic FEA, Optics and Lasers in Engineering 47 (2009) 747-753.

[6] Lava P, Cooreman S, Debruyne D, Study of systematic errors in strain fields obtained via DIC using heterogeneous deformation generated by plastic FEA, Optics and Lasers in Engineering 48 (2010) 457-468.

[7] Wang YQ, Sutton MA, Bruck HA, and Schreier HW, Quantitative error assessment in pattern matching: effects of intensity pattern noise, interpolation, strain and image contrast on motion measurements, Strain 45 (2009) 160-178.

[8] Haddadi H, Belhabib S, Use of rigid-body motion for the investigation and estimation of the measurement errors related to digital image correlation technique, Optics and Lasers in Engineering 46 (2008) 185-196.

[9] Bornert M, et. al. Experimental Mechanics 49 (2009), 353-370.

[10] Sutton MA, Yan JH, Tiwali V, Schreier HW, and Orteu JJ, The effect of out-of-plane motion on 2D and 3D digital image correlation measurements, Optics and Lasers in Engineering 46 (2008) 746-757.

[11] Yoneyama S, Kitagawa A, Kitamura K, Kikuta H, In-plane displacement measurement using digital image correlation with lens distortion correction, JSME International Journal 49 (2006)458-466.

[12] MatchID, Web site: http://www.matchid.org [accessed on 29 February 2012].

[13] Sutton MA, Orteu JJ, Schreier HW. Image correlation for shape, motion and deformation measurements, Springer, New York, 2009.

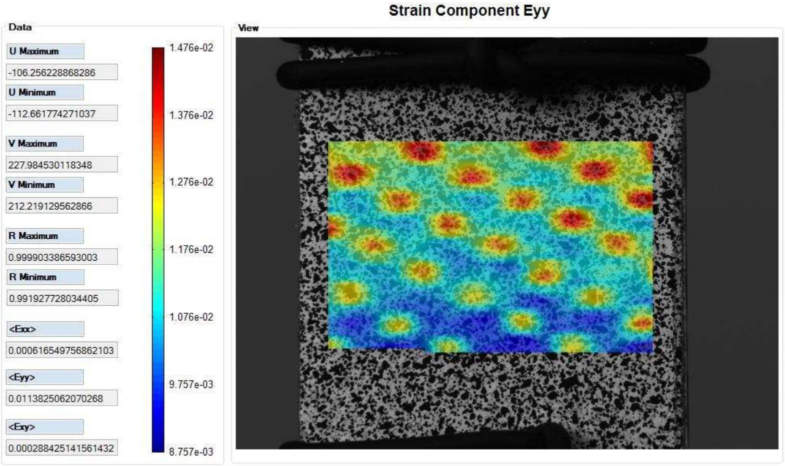

U Maximum
-106.256228868286
U Minimum
-112.661774271037
V Maximum
227.984530118348
V Minimum
212.219129562866
R Maximum
0.999903386593003
R Minimum
0.991927728034405
<Exx>
0.000616549756862103
<Eyy>
0.0113825062070268
<Exy>
0.000288425141561432

Figure 4: Longitudinal strain component for a uni-axial tensile test on a fibre reinforced composite. Results are presented without the inclusion of lens distortion.

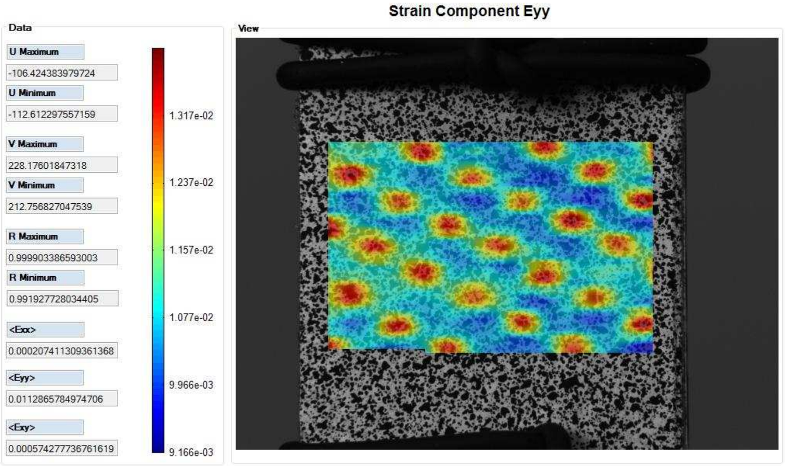

U Maximum
-106.424383979724
U Minimum
-112.612297557159
V Maximum
228.17601847318
V Minimum
212.756827047539
R Maximum
0.999903386593003
R Minimum
0.991927728034405
<Exx>
0.000207411309361368
<Eyy>
0.0112865784974706
<Exy>
0.000574277736761619

Figure 5: Same as in Fig.4 but with lens distortion corrections.

[14] Triggs B, Mclauchlan P, Hartley R, Fitzgibbon A. Bundle adjustment-a modern synthesis. In: Triggs B, Zisserman A, Szeliski R, editors. Vision algorithms. Berlin: Springer;2000.

[15] Lava P, Van Paepegem W, Coppieters S, De Baere I, Debruyne D, *work in progress*.

[16] Lava P, Coppieters S, Wang Y, Van Houtte P, and Debruyne D, Error estimation in measuring strain fields with DIC on planar sheet metal specimens with a non-perpendicular camera alignment, Optics and Lasers in Engineering, 49 (2011) 57-65.